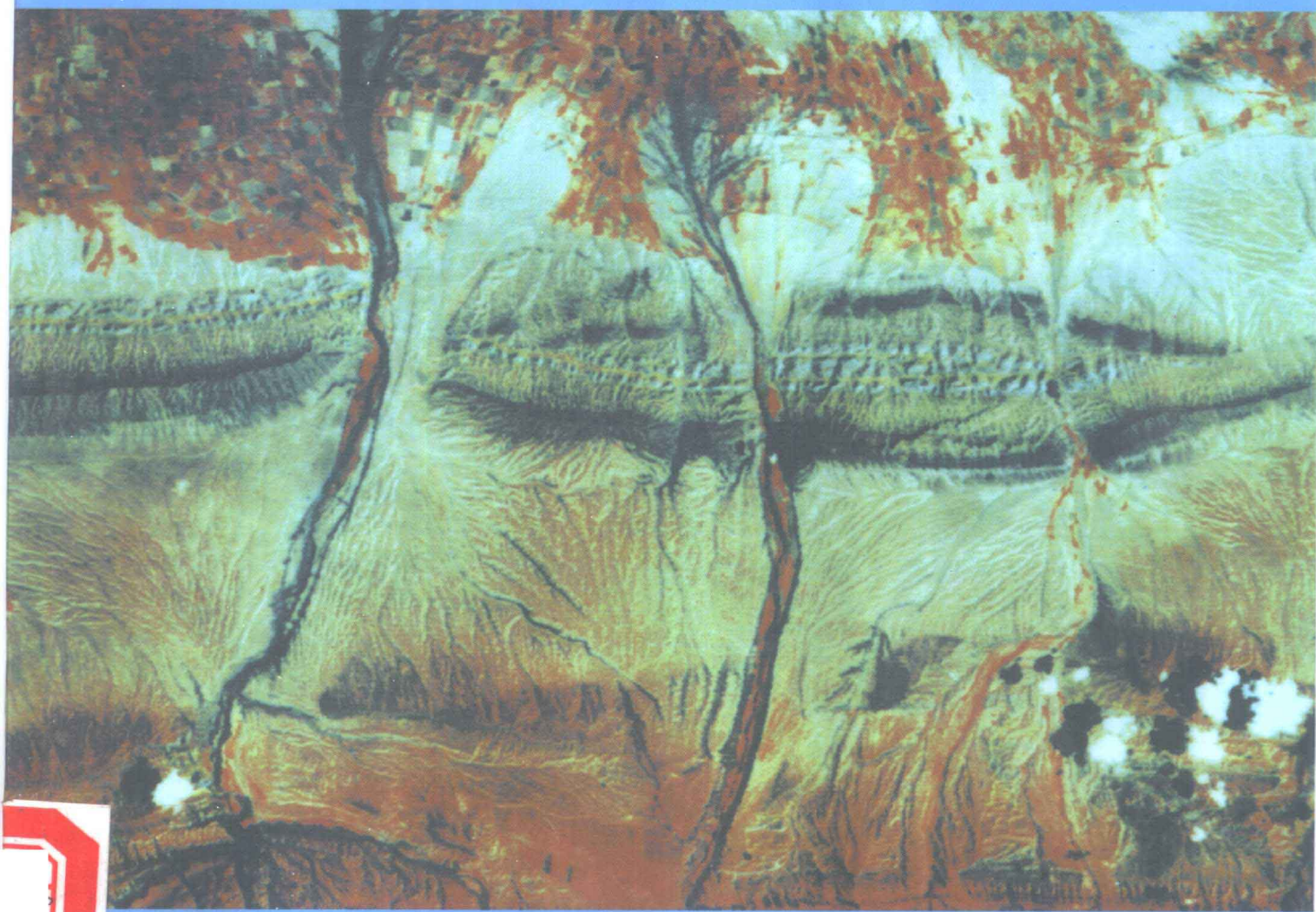


中国活断层研究专辑

天山活动构造

邓起东 冯先岳 张培震 徐锡伟 著
杨晓平 彭斯震 李 军



地震出版社

地震科学联合基金资助
· 中国活断层研究专辑 ·

中国地震局八五重点项目成果
中国地震局地质研究所论著 99F0001 号

天山活动构造

邓起东 冯先岳 张培震 徐锡伟
杨晓平 彭斯震 李 军 著

地震出版社

2000

图书在版编目 (C I P) 数据

天山活动构造 / 邓起东等著. —北京: 地震出版社,
2000.7
ISBN 7-5028-1735-2

I. 天... II. 邓... III. 褶皱带-活动构造-研究-天
山 IV. P548.45

中国版本图书馆CIP数据核字 (2000) 第33845号

天山活动构造

邓起东 冯先岳 张培震 徐锡伟 著
杨晓平 彭斯震 李 军

责任编辑: 李玲

责任校对: 耿燕 庞娅萍

★

地震出版社 出版发行

北京民族学院南路9号

北京地大彩印厂印刷

全国各地新华书店经售

★

787×1092 1/16 26.125 印张 9 插页 669 千字

2000年7月第一版 2000年7月第一次印刷

印数 001—600

ISBN 7-5028-1735-2/P·1036

(2233) 定价: 50.00 元

前 言

宏伟的天山山系绵延耸立于中亚腹地,东起中国境内的新疆维吾尔自治区,西达哈萨克斯坦、吉尔吉斯和塔吉克斯坦等共和国,全长约 2500km,宽度达 250~350km,是亚洲最主要的、规模巨大的年轻山系之一,中国部分的天山横亘于占全国面积 1/6 的新疆维吾尔自治区中部,夹持于准噶尔和塔里木两大盆地之间,东西延伸达 1700km,占天山总长度的 2/3 以上。天山山势雄伟,高耸入云,常年为冰雪所覆盖,平均海拔高度约为 4000m,许多山峰在海拔 5000m 以上,最高峰托木尔峰海拔高度达 7435.3m,屹立于广阔平坦、干燥炎热的荒漠原野间。美丽富饶的天山以其丰富的冰水资源、矿产资源和森林草地资源等哺育着新疆各族人民的同时,也经常引发多种自然灾害,给那里的人民带去不幸,地震灾害就是其中之一。

在漫长的地质历史长河中,早在古生代时期,天山就已经是欧亚大陆中的一条规模巨大的聚合带,经历了多次强烈的地壳变动,但最新的地壳变动则是发生在(3800~4000)万年前印度与欧亚两大板块碰撞后的喜马拉雅构造运动。现今印度板块仍以每年约 50mm 以上的速度向北推进,影响到与之相距 1000 多公里的天山地区(Minster and Jordan, 1978),在印度板块向北推挤这一无可比拟的巨大动力作用下,天山地区的地壳遭受到了强烈的挤压缩短,并再一次强烈抬升,形成了一条规模宏大的年轻的板内再生造山带,即使与号称世界屋脊的青藏高原相比,虽然面积要小得多,但其挤压活动程度、缩短速率和抬升幅度等均毫不逊色。面对自然界这种神奇的造物功能,自古至今人们无止境的感叹和崇拜,并永不停息地去揭开它那若隐若现的神秘面纱。早在先秦至西汉,天山就已由“北山”之谓变成“天山”之称,以抒发先辈们对其崇敬之情;自唐代开始,诸如《大唐西域记》(公元 146 年)、《经行记》(公元 765 年)、《西域水道记》(公元 1823 年)和《冰岭记程》(公元 1861 年)等著作都是古代人们对其不断观察的记实。可以说,神奇的天山永远是一个古老、神奇、充满活力的话题。

在现代科学发展的历史长河中,神秘的天山更是中外地球科学家探索的圣殿,先辈们在人迹罕至的天山及其邻近的广阔沙漠地区留下了他们的斑斑足迹,B. A. 奥布鲁切夫(1892~1909)、袁复礼(1929~1930)和黄汲清(1943)等令人尊敬的科学前辈在天山地区开创性的工作成果至今仍在发出它们的光芒;40 年代初期,苏联学者杜阿耶夫和沙依道夫等已涉足天山地区的地质研究。新中国成立后,神秘天山的面纱逐渐被大规模的地质勘探所揭开。我国地质、石油和其他许多部门的科学家们从 50 年代以来行进于天山南北,攀登在天山山峰和腹地,1:20 万区域地质测量相继进行,石油普查与勘探逐步开展,矿产资源勘探与开发不断扩大,交通和水电工程建设不断发展,地震研究也得到了应有的重视。在这一阶段,多幅 1:20 万区测图件相继出版,涉及不同地学内容的著作不断问世,如《西北地区区域地层表,新疆维吾尔自治区分册》和《新疆自治区地质图》(1:200 万)相继于 1981 和 1985 年出版;有关天山山体演化、构造特征和发展、深部构造、地貌冰川和气候序列、地震地质和地壳形变等多种著作也陆续发表,多方面的研究工作使人们从不同的侧面逐渐地认识了天山,开发着天山(中国科学院地理研究所,1964;彭希龄,1975,1985;新疆地质矿产局,1978;周申喜,1981;乔作山,1981;柏美祥,1981;彭敦复等,1981;张云林,1981;戈树漠,1982;吴裕文等,1982;张良臣和吴乃元,1985;冯

先岳,1985,1986;中国科学院新疆地理研究所,1986;吴庆福,1986;胡军和柏美祥,1988;李秉孝等,1989;文启忠和乔玉楼,1990,李吉均,1990,施雅风等,1990;俞仁连和付恒,1993;彭树森,1993;胥颐等,1994;陈华慧等,1994;中国科学院新疆资源开发综合队,1994)。

值得指出的是,朱海之等由于工程安全评价的需要,1989年首次对北天山山前的晚第三纪—第四纪独山子背斜和断裂进行了很好的研究,对独山子背斜山前逆断裂及斜切独山子背斜的北西向剪切断裂作了研究,包括古地震探槽开挖和年龄测试,对断层的新活动和背斜的构造特征等也作了初步的分析(朱海之和陈杰,1990),这可以说是对本区活动构造第一次进行详细地研究。然而,到目前为止,人们对天山这一现代仍在活动着的活动构造带的许多方面的认识还不清楚,对这一条强烈地震活动带内的地震发生机制依旧茫然。

在广阔的中国大陆上,活动构造的类型十分复杂,既有经受着地壳伸展的拉张区,属正断裂和地堑、半地堑型张性构造系列;也有规模巨大的经受着强烈剪切作用的走滑构造系列;还有遭受强烈挤压使地壳缩短的挤压区,发育着活动褶皱和逆断裂等构造系列。它们在中国大陆上造就了不同类型的自然生态环境和地貌景观,影响着人类的生息繁衍。由于上述构造环境的差异,不同构造环境和类型的地区,其构造几何格局、地壳变形特征、位错方式和动力学过程等都是截然不同的。在过去20年里,活动构造方面的详细研究大多集中在大陆内部的张性构造区和剪切构造带上,而对大陆内部挤压构造及其与大地震的相互关系一直没有机会去详细地加以研究。天山是一个十分典型的大陆内部挤压型活动构造区,是开展这一研究的理想场所。

20世纪80年代,在世界上一些活动挤压构造区相继发生了一些大地震,如1980年阿尔及利亚阿斯南(EL Asnam)7.2级地震,1983年美国科林加(Colinga)6.3级地震,1985年美国凯特曼山(Kettleman Hill)6.1级地震,1987年美国怀特莱露(Whittier Narrows)6.0级地震和1988年前苏联亚美尼亚(Armenian)6.9级地震等。已有的研究表明,这些地震都是挤压构造区受活动盲逆断裂及与其相关的活动褶皱控制的地震,并被命名为“褶皱型地震(Folding - Earthquake)”(Stein and Yeats, 1989)。由此可见,不仅大陆内部挤压构造区的活动构造变形机制和动力学有待我们去研究,一种新类型的地震孕育和发生模型也有待我们去探索,这两方面无论对挤压构造区的地震危险性评估,还是对现代地球动力学的研究都有着十分重要的理论意义和减灾现实意义。

基于上述种种理由,在国家地震局的支持和资助下,我们自1989年开始了天山挤压构造区的活动构造及其与大地震的关系进行研究。1991年,国家地震局“八五”重点地震科学研究计划开始实施,这一研究被列为重点科研项目,项目编号为85-02-1-3。我们的工作涉及到天山南北山前地区及天山内部一些山间盆地的活动构造,包括北天山山前的乌鲁木齐拗陷和南天山山前的库车拗陷及吐鲁番、伊犁、巴鲁布鲁克和焉耆等盆地地区的各种类型的活动构造,并沿独山子—库车和乌鲁木齐—巴仑台—库尔勒横穿天山的公路填制了两条活动构造走廊地质图。天山构造带规模如此巨大,为了使研究工作更加深入,我们在前述工作的基础上,又把主要力量集中在北天山山前和天山内部吐鲁番盆地区,期望以点带面,通过对这两个具有广泛代表性地区活动构造的深入研究,获得对大陆内部挤压型活动构造特征的更深刻认识。为此,我们对北天山山前准噶尔南缘断裂以北前陆盆地内多排活动逆断裂—背斜带和吐鲁番盆地中央隆起带进行了1:5万活动构造地质填图,重点研究活动逆断裂和活动褶皱的变形特征、相互关系及其形成机制,研究它们的最新活动特点和历史、地壳缩短量和缩短速率、大

地震的形成条件和发生机制、地表破裂型古地震的重复间隔,并根据这些活动构造带的多种定量数据对各构造带当前的地震危险性——进行评估,以服务于地震预测、防震减灾和经济建设的需要。

在此期间,我们在 1991~1993 年期间与美国麻省理工学院地球、大气和行星科学系 B. C. 伯奇菲尔(B. C. Burchfiel)和 P. 莫尔纳(P. Molnar)教授在南北天山山前地区开展了活动构造方面的合作研究。先后在天山南北麓实测了若干条走廊地质图(比例尺 1:5 万),并对几条已变形河流阶地和冲洪积扇上最新断层崖用全站仪(Total Station)测制了大比例尺地形剖面 and 平面图(Molnar et al., 1994; Brown et al., 1998)。与此同时,法国巴黎地球物理研究所 T. P. 艾瓦克(T. P. Avouac)与新疆自治区地震局、新疆工学院的柏美祥等也在这一地区对山前逆断层的新活动开展了研究(Avouac et al., 1993);中国地质大学刘和甫、梁慧社等对天山两侧前陆盆地的构造变形和演化开展了研究(刘和甫等, 1994);M. B. 艾伦等对吐鲁番盆地的演化进行了野外考察工作(Allen et al., 1990);此外,我们在 1991 年中国西部石油长输管道活动断裂研究、1994~1998 年多项工程地震安全性评价研究和聂宗笙等(1992)对鄯善地区油田场址地震基本烈度复核研究工作中对天山地区的活动构造都进行过程度不同的研究工作。

我们从 1989 年开始的天山地区挤压活动构造研究工作,历时 6 年,于 1994 年完成了野外 1:5 万活动构造地质填图和多种测量及年龄测试工作,1995 和 1996 年对野外获得的各项资料进行了整理和进一步分析,并最终完成了本研究专著。本书的内容涉及到天山再生造山带不同地段和不同类型的活动构造,资料主要来源于作者多年来在这一最新造山带内的实际调查工作,同时也吸收了前人和同时期研究者的有关成果,除了在第一章中对天山的区域地质条件和区域活动构造作了全面的介绍外,并在有关章节中对北天山山前和吐鲁番盆地两个重点研究区的活动构造、地震构造和古地震及地震危险性等作了详尽的分析,同时,在专门的章节中对天山地区活动构造的几何学和运动学、天山再生造山带的构造恢复和地壳缩短量、天山最新造山带的演化、形成机制和动力学进行了讨论。

参加天山活动构造这一研究工作的单位为国家地震局地质研究所和新疆维吾尔自治区地震局,项目负责人为邓起东、冯先岳和张培震,先后参加过不同阶段工作的人员有徐锡伟、杨晓平、彭斯震、尤惠川、吴章明、于贵华、张宏卫(以上人员为国家地震局地质研究所)、李军、张勇、赵瑞斌、陈杰、杨继林、石鉴邦、李锰、买颜东(以上人员为新疆维吾尔自治区地震局)等。参加本书各章节编写的人员有邓起东、冯先岳、张培震、徐锡伟、杨晓平和彭斯震等,全书由邓起东、徐锡伟和杨晓平等三人负责修改、补充和最终定稿。图件由张兰凤清绘。

全书完成后,由于众所周知的原因,未能及时出版,所幸 1998 年终于得到地震联合基金会的出版资助,批准号为 598003,使本书得以与广大读者见面,所以,在此首先应该感谢地震科学联合基金会。当然,我们应该同时感谢中国地震局对本项目的支持和资助。没有他们的支持,本项工作无法进行,本书也不可能奉献于广大读者面前。此外,在整个研究工作和本书的编写过程中参考和使用了前人大量的地质和地球物理资料,尤其是地质部门 1:20 万区域地质测量资料和石油部门的有关地震探测剖面等,在此亦深表谢意。

Active Tectonics of the Chinese Tianshan Mountain

Abstract

As the most active intracontinental mountain belt in the world, the Tianshan Mountain (literally "Heavenly Mountains" in Chinese) in northwestern China provides an outstanding natural laboratory of studying and understanding intracontinental deformation, a frontier field in today's earth sciences. Lying north of the Tarim basin and Pamir, the Tianshan forms part of a region of post-collisional intracontinental deformation within the India-Eurasia convergent system. The Tianshan extends eastward from southeastern Uzbekistan more than 2000 km to western Mongolia. Maximum elevations in the Tianshan exceed 7000 m and attest to substantial crustal thickening. The earthquake history during the past two centuries, including 5 earthquakes assigned magnitudes as large as 8, demonstrates rapid rates of deformation. Fault plane solutions of earthquakes show that reverse faulting is the principal model of deformation within the upper and middle crust, as is observed in other active intracontinental mountain belts. At the same time, fold and reverse fault belts within sedimentary rocks mark the northern and southern edges of the mountain belt. The Tianshan is therefore serving as a prototype for intracontinental deformation in other part of the world.

The Tianshan Mountain consists of metamorphic, igneous, and sedimentary rocks from Proterozoic to Cenozoic era. These rocks have been intensively folded and faulted to form a very complicated structure pattern suggesting multiple phases of orogeny during geological evolution. The closing of oceanic regions within the Tianshan was in late Carboniferous - early Permian time. The collisional phase of orogeny was probably finished in late Permian, and the Tianshan region started to uplift into mountains. Tectonics during the entire Mesozoic time was relatively weak with respect to Paleozoic time. Mesozoic terrigenous sedimentation deposits along both sides of the Tianshan. The uplifting of modern Tianshan Mountain was probably started since 20 to 24 Ma ago. The significant acceleration of deformation in Chinese Tianshan occurred after 2 Ma. The ragged landscape and active geological structures are products of this latest tectonic deformation in the eastern Chinese Tianshan. The eastern part of Chinese Tianshan is bounded, in a regional scale, by the Zhungaer basin in the north and the Tarim basin in the south. Foreland basins are present along both northern and southern edges of the Tianshan Mountain. We have conducted five-year studies of late Cenozoic deformation along eastern part of the Tianshan with an emphasizing on the reverse fault and fold zones in the Wulumuqi and Tulufan foreland basins. The studies include 1:50,000 scale geological mapping of fold and reverse fault zones, detailed geomor-

phology of rivers and alluvial fans, structural pattern of the range – front fold and reverse zone, paleoseismology along major reverse faults, and earthquake potential of the eastern Tianshan region.

The Wulumuqi foreland basin

There are four rows of reverse fault and fold zones in the Wulumuqi foreland basin. From Tianshan toward Zhungaer basin northward they are the Qigu, the Huoerguosi – Manasi – Tugulu, and the Dushanzi – Hala – ande reverse fault and fold zones. In addition, the Xihu uplift and the Hutubi anticline are growing into the latest row of reverse fault and fold zone. The Qigu reverse fault and fold zone consists of many folds and faults. The youngest stratum involved in the zone is the Xiyu conglomerate of lower Pleistocene. All of the anticlines are asymmetric with steep northern limbs and gentle southern limbs. Reverse faults had developed along the cores or the northern limbs of anticlines approximately parallel to the overall orientation of the Qigu zone. Most of the fault planes dip southward with a few to the north. Geological mapping indicates that the Qigu zone is no longer active at present. The southern marginal fault separating the Tianshan Mountain from the Zhungaer basin has been tectonically inactive since 30,000 years.

The Huoerguosi – Manasi – Tugulu reverse fault and fold zone extends in east – west direction more than 130 km in length, and composed of the Huoerguosi, Manasi, and Tugulu anticlines and their associated reverse faults. Sedimentary rocks involved in the anticlines are lower Tertiary, Miocene, Pliocene, lower Pleistocene, and middle Pleistocene in ages. Similar to the Qigu zone, anticlines in the Huoerguosi – Manasi – Tugulu zone also are asymmetric with steep or overturned northern limbs and gentle southern limbs. The Huoerguosi – Manasi – Tugulu zone was probably initiated at the end of Pliocene or the beginning of early Pleistocene, as demonstrated by a slight unconformity between Pliocene and early Pleistocene sedimentary rocks. Since a clear angular unconformity exists between lower and middle Pleistocene, major phase of deformation along this zone must occur during this time interval. Many southward dipping reverse faults have developed along the cores or northern limbs of the anticlines in the zone with dip angles of $40^{\circ} \sim 50^{\circ}$. Reverse faults are associated with each anticline. Some of them displace the core of anticline such as the case of Tugulu, and others develop along the northern limbs of the anticline. The steep to overturned northern limbs and south – dipping reverse faults attest to northward convergence of the Huoerguosi – Manasi – Tugulu reverse fault and fold zone.

The Dushanzi – Hala – ande reverse fault and fold zone is about 80 km in length. It consists of the Dushanzi, Hala – ande, and Anjihai anticlines and their associated reverse faults. The core of Dushanzi is composed of early Miocene and Pliocene sedimentary rocks, and the limbs are lower Pleistocene conglomerates. In Anjihai and Hala – ande anticlines, the earliest rocks exposed in the core are Pliocene yellowish sandstone and conglomerate. Reverse faults mostly crop out along the northern limbs of the anticlines. In general, southern limbs of the anticlines are gentler dipping than the northern limbs. There is no overturned northern limb. The convergence in this zone is also toward the north, but the intensity of deformation is much less than the reverse fault and fold

zones in the south. Fault scarps presented along this reverse fault and fold zone indicate modern tectonic activity.

The Tulufan foreland basin

The Tulufan foreland basin is located along the southern edge of modern Tianshan Mountain. The foreland basin is probably formed since Cenozoic time as the tectonic activity migrates from south of the Juluotage highland to the range – front of Bogeda Mountain, the modern body of the Tianshan east of Wulumuqi. The Tulufan basin is filled with Mesozoic to Cenozoic terrestrial sediments. The absence of angular unconformity from Cretaceous to lower Pleistocene suggests that there is no significant deformation taken place during this time span in the Tulufan foreland basin although increase of depositing rate in Miocene is viewed as onset of deformation and crustal shortening in responding to Indian – Eurasian collision. The youngest sediments involved in folding in Tulufan basin is lower Pleistocene Xiyu conglomerate that suggests significant deformation occurred after early Pleistocene time.

Structures controlling formation of the Tulufan basin are the Bogeda range – front fault and the central – basin structural zone. The Bogeda range – front fault zone consists of a series of north – dipping reverse faults with relatively high angles from 50° to 70° forming a southward converging zone. As tectonic activity migrated from the Bogeda range – front fault to the central – basin structural zone during Quaternary, normal faults developed along the range front that cut preexisting reverse fault.

The central – basin structural zone consists of three anticlines and associated reverse faults. From west to east they are the Yanshan, the Kendeke, and the Fire Mountain anticline. Orientation of the central – basin structural zone is parallel to the main trend of the Tianshan Mountains. The oldest rocks cropped out in the core of these anticlines are Cretaceous sandstone and mudstone. Tertiary red beds and lower Pleistocene Xiyu conglomerate form northern limbs of these anticlines. The southern limbs are usually absent because of fault displacement in most places of these anticlines. Where the southern limbs are present, they either overturned to the north or they steeply dip to the south or vertical. Reverse faults are present on southern side of the central – basin structural zone because they usually destroy the southern limbs of those anticlines. The geometric pattern and sense of reverse faulting in the Tulufan basin suggest southward convergence.

The Kuche foreland basin

Although the Kuche basin is out of our study area we still conducted some researches because it is another major foreland basin in the eastern Tianshan. Thick sequence of Cenozoic sediments has been intensively folded and faulted. Three unconformities are found in the sequence, which are that between lower Tertiary and Mesozoic, Pliocene and Lower Pleistocene, and middle and lower Pleistocene rocks. Among them, the tectonic event occurred between middle and early Pleistocene epoch is most important one that creates primary Cenozoic tectonic framework and

pattern of modern geomorphology.

There are four rows of reverse fault and fold zones in the Kuche foreland basin. The range-front reverse fault and fold zone forms boundary structure between Tianshan Mountain and Kuche foreland basin. Paleozoic rocks on the hanging wall thrust to the south along the zone. Folds cored by Mesozoic rocks also developed in association with the reverse fault. The Hasangtuokai reverse fault and fold zone is the second row from north. Anticlines in this zone show steep to overturned southern limbs and gentle northern limbs. Reverse faults often offset southern limbs and destroy them. The Qiulitage reverse fault and fold zone is the major structure in the Kuche foreland basin. It extends for about 250 km parallel to the Tianshan Mountain. The Qiulitage zone consists of 14 anticlines with steep or overturned southern limbs. Geometric pattern of the anticlines and sense of motion on the thrust faults indicate southward convergence of the Qiulitage zone. The Yaken anticline, a gentle uplift in modern geomorphology, is the fourth and the southernmost row of reverse fault and fold in the Kuche foreland basin. Geological mapping reveals that the strata on both limbs dip 5 to 10° and is therefore a newly growing anticline similar to the Xihu and Hutubi uplifts in the Wulumuqi foreland basin.

Timing of Cenozoic deformation in the Tianshan

It is general agreement that the late Cenozoic rejuvenation of Tianshan Mountain in the intra-continental setting results from collision and subsequent penetration of India into Eurasia. Both uplifting of mountain range and subsidence of foreland basins as well as tectonic deformation are the results of this rejuvenation. Our studies indicate that the Tianshan has subjected to two major phases of deformation. The first phase is uplifting and erosion in the Tianshan Mountain and deposition of terrestrial sediments in the foreland basins. The second phase is thrusting of the Tianshan Mountain onto the Tarim and Zhungar basins and associated broad folding and reverse faulting in all foreland basins surround the Tianshan Mountain.

According to studies on sedimentation in eastern Tianshan, unconformity between Oligocene deposits and underlain rocks is viewed as initiation of uplifting in the eastern Tianshan. Thickness of Cenozoic sediments in the foreland basins show that rate of sedimentation started to increase from Miocene time, and continue upward to reach the maximum in early Quaternary. In the Kashi foreland basin in the Western Tianshan, marine sediment environment ended and terrestrial deposition started in Miocene time. Thus, the first phase of major deformation in the Tianshan may start in Miocene time, which is in a good agreement with fission track and thermochronological studies.

The second phase is probably most important Cenozoic deformation in the Tianshan when the mountain ranges thrust both southward and northward onto the foreland basins. The foreland basins themselves are also subjected significant crustal shortening to form a serious reverse fault and fold zones. According to stratigraphic relationships and the youngest rocks involved in this phase of deformation, this intensive deformation occurred after formation of the lower Pleistocene Xiyu formation and before deposition of middle Pleistocene sediments. Strong earthquakes and modern

crustal deformation along both sides of Tianshan are continuation of this phase of deformation.

Style of late Cenozoic deformation in the Tianshan

Two kinds of deformation, thin-skinned and thick-skinned, are observed in the eastern Tianshan. Thick-skinned structures are present outside foreland basins, for example, Kuerle area east of the Kuche foreland basin along the southern Tianshan, and the Sikeshe area west of the Wulumuqi foreland basin along the northern Tianshan. The Tianshan Mountains thrust onto both Tarim and Zhunga-er basins along high angle reverse faults. There is no reverse fault and fold zone developed inside basin.

The thin-skinned structures characterize deformation in all foreland basins. The reverse fault and fold zones are basically fault-propagation folds. In responding to regional compression, the Tianshan thrusts toward both sides along lower angle decollements. The decollement is usually located several to more than ten kilometers below the surface. As the compression progresses, the decollement propagates into foreland basin from below. It usually ramps upward to form a row of reverse fault and fold on the surface. With continuation of deformation, the decollement propagates again, and may ramp upward to form another row of reverse fault and fold. As this kind of process goes on, several rows of reverse fault and fold may form in foreland basin. In the Wulumuqi foreland basin for example, there are two decollement surfaces, and each has been associated with two ramps and two anticlines. The lower decollement is located in Jurassic sediment rocks about 8 to 9 km below the surface. Qigu reverse fault and fold zone developed on top of the lower ramp. The Huoerguosi-Manasi-Tugulu reverse fault and fold form on top of the second anticline. The upper decollement is located in low Tertiary rocks at depth about 3 to 4 km. It merges downward into the lower decollement surface. The first ramp of upper decollement is associated with the Huoerguosi-Manasi-Tugulu reverse fault and fold zone. The two decollements form a duplex structure beneath the Huoerguosi-Manasi-Tugulu reverse fault and fold zone. The second ramp of the upper decollement cropped out on the surface to form the Dushanzi-Hala-ande-Anjihai reverse fault and fold zone. The decollements may continue propagating northward. The Xihu uplift and the Hutubi uplift may be representations of thrust ramps at depth.

Quantitative estimation of Quaternary crustal shortening

Amounts of crustal shortening across the Tianshan are an important aspect in study of kinematics and geodynamics. There are three methods to estimate crustal shortening: geological mapping and balanced cross-section restoration, deducing from late Quaternary slip rate, and calculation from theoretical models. According to our geological mapping, we have calculated crustal shortening in the Tulufan, Wulumuqi, and Kuche foreland basins by technique of balanced cross-section. The amounts of shortening in the three foreland basins are 10-12 km, 17 km, and 23 km respectively. Crustal shortening in the Kashi foreland basin is 23-50 km based on previous study. These amounts represent minimum Quaternary crustal shortening across the Tianshan because deformation with the Tianshan Mountain has not accounted for. The amounts show that the

distribution of crustal shortening decreases from west to east. This pattern is in agreement with the qualitative estimation by the thickness of Cenozoic sedimentation and results computed from theoretical model.

There are many rivers across the reverse fault and fold zones in the foreland basins. Terraces are developed inside these river valleys. There are usually two levels of terraces along the major river valleys. In the minor rivers the valleys usually have one continuous terrace. Where the rivers cross the reverse fault and fold zones, the terraces have been folded to form gentle anticlines, the numbers of terraces has been increase, and the type of terrace has been changed from deposition to strath. All of these reflect impacts of continued folding to formation of river terraces. By dating the folded and faulted terraces the late Pleistocene slip rates are $4 \sim 11$ mm/yr and $4.9 \sim 9$ mm/yr for the Wulumuqi and Tulufan foreland basins respectively.

Paleoseismology and seismic hazard assessment

The eastern Tianshan Mountain is also an earthquake prone region. In 1906 an earthquake with magnitude $M_s = 7.7$ occurred along northern range – front of Tianshan in the Wulumuqi foreland basin. Detailed field mapping discovers that surface ruptures associated with the earthquake are only less than 10 km in length and coseismic displacements are less than 0.5 m. These parameters are not comparable with the 7.7 magnitude earthquake. Field studies also reveal an about 130 km slightly uplifted zone. This uplifted zone is probably associated with the 1906 Manasi earthquake. The Manasi earthquake itself was a "folding earthquake" similar to the 1983 Colinga earthquake in California, U.S.A.

To study earthquake potential in the eastern Tianshan, trenches have been dug across reverse faults along both northern and southern sides of Tianshan. Many paleoseismic events have been discovered from these trenches. The recurrence intervals along different reverse fault and fold zones are different. The average recurrent interval during last 20,000 years is about 4000 years along the Dushanzi – Hala – ande reverse fault. The elapsed time along this zone however is also about 4000 years. Thus, this zone has large potential for future large earthquake. Average recurrence interval along the Huoerguosi – Manasi – Tugulu zone is measured to be 5000 – 6000 years, and it therefore has less potential for future large earthquake because of the 1906 Manasi earthquake. In the Tulufan foreland basin, the average recurrence interval is about 3000 years. The elapsed time since last paleoearthquake is about 2500 years. Thus, there is also potential in the Tulufan basin for future large earthquake.

目 录

前言	(1)
第一章 区域地质构造背景	(1)
第一节 天山地区的地层与沉积作用	(1)
第二节 天山地区的岩浆活动和变质作用	(13)
第三节 区域地质构造及演化历史	(17)
第四节 区域地球物理场特征及深部构造	(24)
第五节 区域地貌特征	(31)
第六节 现代地壳形变特征及地震活动性	(37)
第七节 天山地区主要活动构造带	(42)
第八节 构造应力场	(74)
第二章 北天山山前的活动构造	(77)
第一节 准噶尔南缘断裂及其活动性	(77)
第二节 山麓逆断裂—背斜带的变形特征	(81)
第三节 霍尔果斯—玛纳斯—吐谷鲁逆断裂—背斜带的变形特征	(88)
第四节 独山子—安集海逆断裂—背斜带的变形特征	(127)
第五节 西湖隆起的变形特征	(147)
第三章 吐鲁番盆地的活动构造	(148)
第一节 基本地貌单元及其编年	(148)
第二节 盆地周缘的活动断裂	(157)
第三节 中央隆起构造带的地质构造变形特征	(163)
第四节 晚新生代构造演化历史	(185)
第四章 天山活动构造的几何学和运动学特征	(188)
第一节 挤压构造区的构造变形组合	(188)
第二节 北天山山前断展褶皱的几何学和运动学特征	(199)
第三节 吐鲁番盆地中央隆起带断展褶皱的几何学和运动学特征	(213)
第四节 山前逆断裂—背斜带及山间盆地的形成机制	(220)
第五章 天山活动构造带的构造恢复和地壳缩短量	(251)
第一节 北天山中段山前活动逆断裂—褶皱带的地壳缩短量	(251)
第二节 南天山中段山前活动逆断裂—褶皱带的地壳缩短量	(257)
第三节 吐鲁番盆地的地壳缩短量	(260)
第四节 天山活动构造带地壳缩短量的讨论	(261)
第六章 北天山山前和吐鲁番地区晚更新世以来褶皱变形的定量研究	(266)
第一节 北天山山前地区晚第四纪河流阶地的发育和结构特征	(266)
第二节 北天山的冰水冲洪积地貌及其编年	(273)

第三节	吐鲁番盆地地貌单元及其编年·····	(279)
第四节	晚第四纪气候、地貌单元及其成因·····	(283)
第五节	晚更新世褶皱变形测量的基本原理·····	(288)
第六节	北天山山前逆断裂—背斜带晚更新世以来褶皱变形的定量研究·····	(290)
第七节	吐鲁番盆地中央隆起带晚更新世以来的逆断裂—褶皱作用·····	(299)
第七章	1906 年玛纳斯地震的地表形变、破裂机制与发震模式·····	(302)
第一节	盲逆断裂—褶皱型地震·····	(302)
第二节	1906 年玛纳斯地震极震区地表破坏研究·····	(303)
第三节	玛纳斯地震区的活动断裂·····	(306)
第四节	呼图壁断层陡坎几何学和运动学特征·····	(308)
第五节	玛纳斯与霍尔果斯最新断裂陡坎·····	(314)
第六节	呼图壁、玛纳斯和霍尔果斯逆断裂最新陡坎的成因·····	(315)
第七节	1906 年玛纳斯地震产生的最新隆起带·····	(317)
第八节	玛纳斯地震的形成模式与机制·····	(320)
第八章	北天山山前地区和吐鲁番盆地的古地震研究·····	(322)
第一节	独山子—安集海逆断裂—背斜带的古地震探槽研究·····	(323)
第二节	霍尔果斯—玛纳斯—吐谷鲁逆断裂—背斜带的古地震研究·····	(329)
第三节	吐鲁番盆地中央隆起带逆断裂的古地震研究·····	(339)
第四节	有关逆断层古地震标志的讨论·····	(344)
第九章	北天山山前地区和吐鲁番盆地地震危险性评价·····	(348)
第一节	活动断裂地震危险性定量评价的思路与方法·····	(348)
第二节	天山地区地震活动概况及其发震构造评价·····	(354)
第三节	北天山地区的古地震与地震危险性评估·····	(359)
第四节	北天山地壳缩短速率与地震危险性评估·····	(360)
第五节	大地震重复周期及地震危险性概率评价·····	(363)
第六节	北天山地区大地震危险性的综合评估·····	(369)
第十章	天山地区的晚新生代构造变形及其地球动力学问题·····	(373)
第一节	天山构造变形简史·····	(373)
第二节	新生代构造变形的基本特征·····	(375)
第三节	天山新生代变形的地球动力学问题·····	(382)
结束语	·····	(386)
参考文献	·····	(387)

Contents

Preface	(1)
1 Regional geological setting	(1)
1.1 Stratum and sedimentation	(1)
1.2 Magmatism and Metamorphism	(13)
1.3 Regional tectonics and its evolution	(17)
1.4 Regional geophysical field and crustal structure	(24)
1.5 Regional geomorphic features	(31)
1.6 Modern crustal deformation and Seismicity	(37)
1.7 Major active tectonic belts	(42)
1.8 Tectonic stress field	(74)
2 Active tectonics along the piedmont of North Tianshan	(77)
2.1 Southern marginal fault of Dzungaria basin	(77)
2.2 Northern Tianshan piedmont reverse fault – fold belt	(81)
2.3 Huoerguoc – Manas – Tugulu reverse fault – fold belt	(88)
2.4 Dushanzi – Anjihai reverse fault – fold belt	(127)
2.5 Deformation of Xihu uplift	(147)
3 Active tectonics of Turpan Basin	(148)
3.1 Basic geomorphic units and their chronology	(148)
3.2 Active faults around Turpan basin	(157)
3.3 Tectonic deformation of central uplift belt	(163)
3.4 Structure evolution in Later Cenozoic	(185)
4 Geometry, kinematics of active tectonics in Tianshan	(188)
4.1 Deformation pattern in compressional region	(188)
4.2 Geometry and kinematics of fault – propagation folds in North Tianshan piedmont	(199)
4.3 Geometry and kinematics of fault – propagation folds in Turpan basin	(213)
4.4 Mechanism of range – front reverse fault – fold belt and intermontane basin	(220)
5 Structural restoring and crustal shortening of Tianshan active tectonic zones.	(251)
5.1 Crustal shortening of the active reverse fault – fold belt in North Tianshan piedmont	(251)
5.2 Crustal shortening of the active reverse fault – fold belt in South Tianshan piedmont	(257)
5.3 Crustal shortening of Turpan basin	(260)

5.4 Discussion on crustal shortening in Tianshan region	(261)
6 Quantitative research on fold deformation in North Tianshan region since Late Pleistocene	(266)
6.1 Late Quaternary river terrace and frame features along North Tianshan	(266)
6.2 Glaciofluvial geomorphology and its chronology in Northern Tianshan	(273)
6.3 Geomorphic units and their chronology for Turpan basin	(279)
6.4 Late Quaternary climate changes, geomorphic units and their origin	(283)
6.5 Basic principle for fold deformation measuring since late Pleistocene	(288)
6.6 Quantitative research on fold deformation along reverse fault – fold zones in North Tianshan piedmont	(290)
6.7 Late Quaternary reverse faulting and folding along the central uplift belt in Turpan basin	(299)
7 Surface deformation, faulting mechanism and seismogenic model for 1906 Manas earthquake	(302)
7.1 Blind thrust and fold earthquake	(302)
7.2 Surface rupture pattern in meizoseismal region of 1906 Manas earthquake	(303)
7.3 Active faults in the 1906 Manas earthquake region	(306)
7.4 Geometry and kinematics of Hutubi fault scarps	(308)
7.5 Youngest fault scarps along Manas and Huoerguos reverse fault – fold zone	(314)
7.6 Formation origin for the youngest fault scarps along Hutubi – Manas – Huoerguos reverse fault zone	(315)
7.7 Youngest uplift zone for the 1906 Manas earthquake	(317)
7.8 Faulting mechanism of the 1906 Manas earthquake	(320)
8 Paleoequake research in North Tianshan	(322)
8.1 Paleoequake research on the Dushanzi – Anjihai reverse fault – fold zone ...	(323)
8.2 Paleoequake research on the Huoerguos – Manas – Tugulu reverse fault – fold zone	(329)
8.3 Paleoequake research on the central uplift belt in Turpan basin	(339)
8.4 Discussion on paleoequake indicators for reverse faulting	(344)
9 Seismic risk evaluation for the North Tianshan	(348)
9.1 Quantitative seismic risk evaluation on active fault: Theory and methods	(348)
9.2 Seismic activity and seismogenic structure in Tianshan region	(354)
9.3 Paleoseismicity and seismic risk evaluation	(359)
9.4 Crustal shortening rate and seismic risk evaluation	(360)
9.5 Earthquake recurrence intervals and probabilistic risk evaluation	(363)
9.6 Comprehensive evaluation of earthquake risk for the North Tianshan region ...	(369)
10 Late Cenozoic tectonic deformation and its geodynamics in Tianshan Mountains. ...	(373)
10.1 Brief history in tectonic deformation	(373)
10.2 Basic characteristics of tectonic deformation in Cenozoic	(375)

10.3 Cenozoic tectonic deformation and its geodynamics in Tianshan Mountains ...	(382)
Conclusions	(386)
References	(387)
Photographs	